[8] Bachelet Y, Bourdel S, Gaubert J. Fully integrated CMOS UWB pulse generator. *Electron Lett.* 2006;42:1277–1278.

[9] Bourdel Gainert S, Fourquin J, Vauche O, Dehaese RN. CMOS UWB pulse generator co-designed with package transition. *IEEE RFIC Symp.* 2009; 539–542.

[10] Mai Khanh NN, Iizuka T, Asada K. A damping pulse generator based on regenerated trigger switch. *IEEE RFIC Symp.* 2016; 11–14.

How to cite this article: Tang X, Huang F, Wang X, Chang T, Zhang Y. Ultra-short pulse generator using 0.13-μm CMOS. *Microw Opt Technol Lett.* 2017;59:3094–3097. https://doi.org/10.1002/mop.30884

Received: 18 May 2017

DOI: 10.1002/mop.30882

A microstrip photonic crystal bandgap device with a switchable negative epsilon plasma element

B. Wang | **R. Lee** | **R. Colon** | **M. A. Cappelli**

Department of Mechanical Engineering, Stanford Plasma Physics Laboratory, Stanford University, California 94305

Correspondence
Mark Cappelli, Stanford Plasma Physics Laboratory, Department of Mechanical Engineering, Stanford University, Stanford, California 94305, USA.
Email: cap@stanford.edu

Funding information
Multidisciplinary University Research Initiative from the Air Force Office of Scientific Research; National Defense Science and Engineering Graduate Fellowship

Abstract

We present a microstrip photonic bandgap (PBG) device with a switchable plasma element integrated into the patterned ground plane. A pulsed laser plasma is generated in one of the PBG cavity structures creating a medium having an effective negative permittivity in the 8–10 GHz frequency range due to the high plasma density $n_e = 10^{17}$ cm^{-3}. The PBG structure consists of a linear array of seven cavities along the length of the microstrip manufactured by removing cylindrical portions of copper in the ground plane. The plasma is produced in the central cavity of the PBG array and recombines over times of several microseconds allowing for the characterization of the microstrip transmission over a range of plasma density. The results confirm a switchable transmission due to plasma interactions with the electromagnetic field within the PBG structure.

KEYWORDS

electromagnetic interaction, laser, microstrip, photonic bandgap, plasma

1 | INTRODUCTION

Switchable devices for the high bandwidth control of electromagnetic waves is a major challenge for high powered signals. We have shown in earlier studies that plasma discharges can provide this dynamic control through the integration of active plasma elements in a free space solid state photonic crystal structure.[1] The plasma acts as a tunable dielectric element within the photonic crystal. We have extended the use of active plasma elements into the construction of a full plasma-based photonic crystal, using the active tunability of the plasma to allow for reconfigurability of the wave propagation characteristics. This article presents the integration of a plasma element into a planar microstrip transmission line for the control and manipulation of electromagnetic waves that are confined to a surface of the planar microstrip.

The electromagnetic fields in microstrip devices have TEM propagation modes, which are generally confined to the dielectric regions between the powered microstrip and ground plane. Photonic bandgap (PBG) structures have been integrated into microstrip devices by patterning the ground plane with a 2-D crystal lattice structure.[2,3] The structuring of the ground plane forms PBGs by changing the electromagnetic field that extends into and just beyond the patterned ground plane. The device presented in this article uses a pulsed laser to generate a plasma element within the PBG patterned structure, thereby allowing for active switching of the transmission characteristics. The switching of the device is based on manipulating the fields that extend through the ground plane into the air interface within cavities patterned into the copper ground plane. The plasma is formed within a single cavity of the PBG structure and acts as an active element that generates a dissipative defect with a material that has an effective permittivity $\varepsilon < 0$ changing the transmission properties of the PBG device. In this configuration, the plasma is never in direct contact with the signal line in the device in turn allowing the device to be actively reconfigured. The plasma is in contact with the composite laminate on the ground plane side so there is no damage of the signal

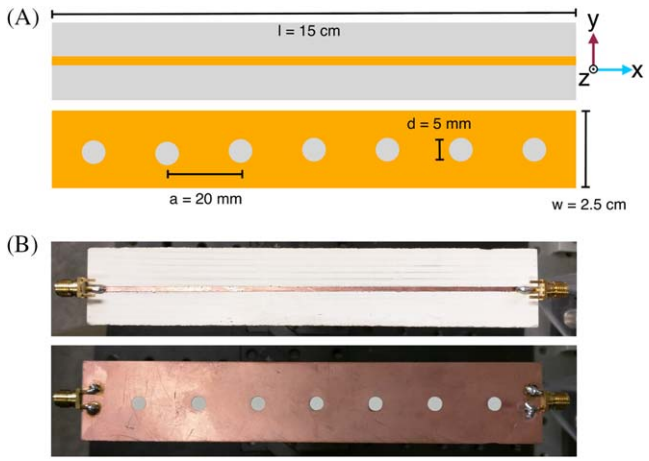

FIGURE 1 A, Schematic of the microstrip device with PBG structure. B, Photograph of the top and bottom of the microstrip device. SMA connectors are attached to the top microstrip. [Color figure can be viewed at wileyonlinelibrary.com]

line and minimal damage to the ground plane when the laser is properly aligned and configured.

Microwave circuits that are based on microstrip designs are generally composed of a variety of active and passive components. A standard microstrip transmission line geometry consists of a signal line on one side of a planar substrate and a ground plane on the other. Planar passive elements are components that are made from changing the physical geometry of the microstrip to form various shapes that allow for the microstrip to act as resistors or capacitors. Active circuit elements include transistors, amplifiers, and oscillators. Previous microstrip devices that have incorporated plasma discharges for tunability have included direct integration into the signal line with the plasma acting as a switchable conducting element[4] or as a tunable circuit element with a variable capacitance and resistance.[5] The microstrip device presented in this letter uses a plasma element together with a photonic crystal bandgap structure to control the microstrip transmission properties.

2 | DESIGN OF PBG MICROSTRIP

A schematic and photograph of the microstrip PBG device is shown in Figure 1. The device was fabricated from a Rogers TMM 10i substrate which consists of a copper-plated thermoset ceramic/polymer composite ($\varepsilon = 9.8$, thickness = 1.27 mm, copper thickness = 35 μm) using a CNC PCB mill. The signal line width is 1.5 mm (resulting in a line impedance of $\sim 50\ \Omega$). The two-dimensional PBG structure is a linear arrangement of seven cylindrical-shaped cavities fabricated by milling away the copper plating on the ground plane. The cavities have a radius $r_h = 2.5$ mm with a lattice constant $a = 20$ mm aligned with the centerline of the microstrip on the ground plane, allowing for the device to have a bandgap between 8 and 9 GHz. Other relevant dimensions are shown in Figure 1. A 190 ± 10 mJ pulse from a Q-switched flashlamp-pumped Nd:YAG laser (SpectraPhysics Quanta Ray PIV-400, pulse width = 8 ns, $\lambda = 1064$ nm) was used to generate the plasma in atmospheric air. The laser was focused ~1 mm above the surface of the ground plane of the center cavity in the photonic crystal bandgap structure. A photograph of the experimental set up with the laser plasma formed in the central cavity is shown in Figures 2 and 3. The microstrip device was placed on a vertical micrometer stage to allow for control of the location of the patterned ground plane relative to the laser generated plasma. A microwave generator (HP 83732A) was connected to the input of the microstrip device, with a crystal detector (Krytar 303SK ZBS) connected to the output port. A data acquisition system allowed for the frequency to be swept from 8 to 10 GHz, and the output of the crystal detector was connected to an oscilloscope (Rigol DS1053Z) to record the transient signal from the detector (from $t = 0$ to $t = 500$ ns following the initiation of the laser pulse). The effect of the temporally evolving plasma density was characterized by measuring the time-varying transmission of the signal as recorded by the crystal detector.

Simulations of the device and its performance were conducted using the commercially available finite element method solver, ANSYS HFSS 16.1. The plasma was simulated as a uniform cylinder of radius $r_p = r_h = 2.5$ mm with a plasma having height $h_p = 2$ mm. The plasma density, n_e was simulated at $3 \times 10^{17}\text{cm}^{-3}$ and $5 \times 10^{17}\text{cm}^{-3}$ both with an electron collision frequency of 100 GHz which are characteristic of atmospheric pressure laser plasmas during the first microsecond of their decay.[6] Simulations were completed using the first order basis function solver, with a

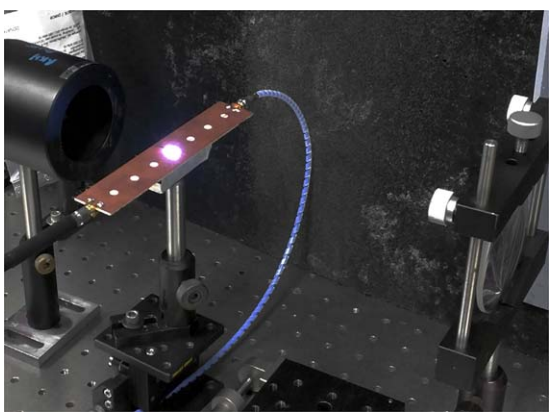

FIGURE 2 Experimental setup with the pulsed laser focused on the center PBG hole of the microstrip device. [Color figure can be viewed at wileyonlinelibrary.com]

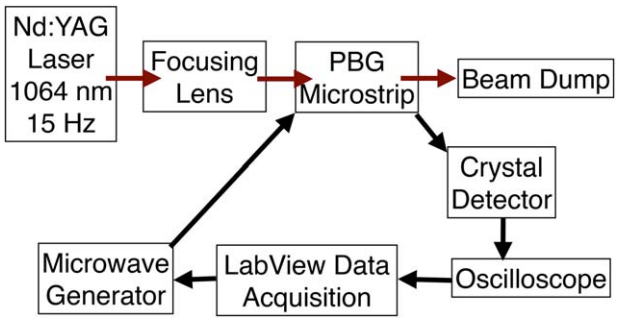

FIGURE 3 Schematic of the experimental and measurement setup of the 1064 Nd: YAG laser induced plasma and microstrip system. [Color figure can be viewed at wileyonlinelibrary.com]

convergence criteria for the maximum change in S-parameters between adaptive passes set at 5%.

The electromagnetic properties of the plasma formed in the cavity of the microstrip were modeled using a frequency-dependent dielectric constant expressed by the usual Drude formula,

$$\varepsilon_p(\omega) = 1 - \frac{{\omega_p}^2}{\omega^2 - i\gamma\omega}$$

with γ is the electron collision frequency (taken to be a constant) and ω_p the plasma frequency,

$$\omega_p = \sqrt{\frac{n_e e^2}{m_e \varepsilon_o}}$$

Here, e is the electron charge, m_e is the electron mass, n_e is the electron density of the plasma, and ε_o is the vacuum permittivity. We see that the dielectric constant of the plasma can be either negative, zero, or positive (but <1), depending on the relative magnitudes of the field frequency, plasma frequency, and collision frequency. Using a pulsed laser generated plasma, a plasma density of $n_e = 10^{17}\text{cm}^{-3}$, anticipated within the first 100 ns, and a collision frequency of $\sim$100 GHz results in a negative permittivity regime of the plasma element since $\omega \ll \gamma \ll \omega_p$. This causes the plasma to act as a lossy negative epsilon element within the ground plane PBG structure.

The interaction between the laser induced plasma and the surface of the microstrip is complex and will be explored in detail in future work. The laser-generated plasma expands as it generates shockwaves that propagate radially from the location of the initial plasma kernel. The expansion of the initially very high density plasma creates a temporally decaying plasma density for the duration of the plasma lifetime and allows for density-dependent temporal characterization of the response of the device. Laser generated plasmas in air using similar pulsed energy and duration have been extensively characterized through shadowgraph imaging and have shown to have a spherical expanding shockwave over a lifetime of 1–2 μs with the core dense plasma having a lifetime of up to 500 ns.[7] The measured plasma properties for the laser-induced plasma in this particular experiment will be discussed in detail in future work. Preliminary results that we have obtained for experiments with a laser-induced plasma in argon at comparable pulse energies and gas pressures show plasma densities and plasma lifetimes on the same order of magnitude as those presented in the studies of Thiyagarajan et al.,[6] justifying the range of values used in the present discussion and in the simulations.

3 | SIMULATION AND EXPERIMENTAL MEASUREMENT RESULTS

The experimentally measured S_{21} parameter, as seen from the transmission spectra depicted in Figure 4, show the effect that the plasma has on the bandgap behavior, with increased signal propagation within the bandgap when the plasma is introduced. At a time of $t = 200$ ns after the initial formation of the plasma, transmission within the bandgap is increased by more than 10 dB when compared with the baseline value (at $t = 0$) obtained in the absence of the plasma just before the firing of the laser. At a time $t = 500$ ns, the plasma is expected to have decayed substantially, evidenced by the reduction in transmission to a value within a few dB of that of the baseline case. The change in structure on the high frequency edge of the bandgap is particularly interesting, as waves propagating in the range of 9–9.5 GHz will see nearly unattenuated transmission (from as low as a 15 dB level of attenuation) when the plasma is ignited.

Figure 5 shows results of the simulated S_{21} parameter of this microstrip device for a baseline condition (no plasma) and two plasma conditions, chosen to illustrate the sensitivity of the mid-gap propagation to electron density. The

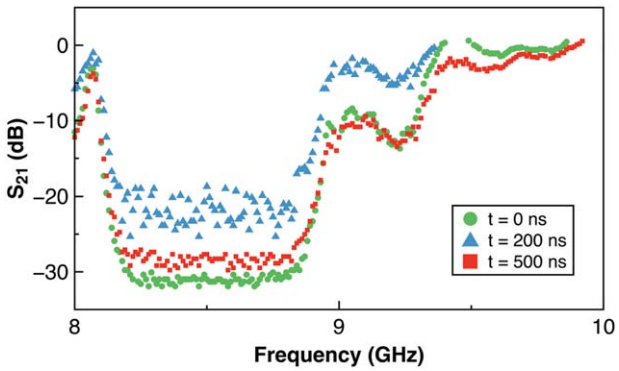

FIGURE 4 Measured S_{21} for the PBG microstrip at time $t = 0$, 200, and 500 ns referenced to the Q-switch of the laser. [Color figure can be viewed at wileyonlinelibrary.com]

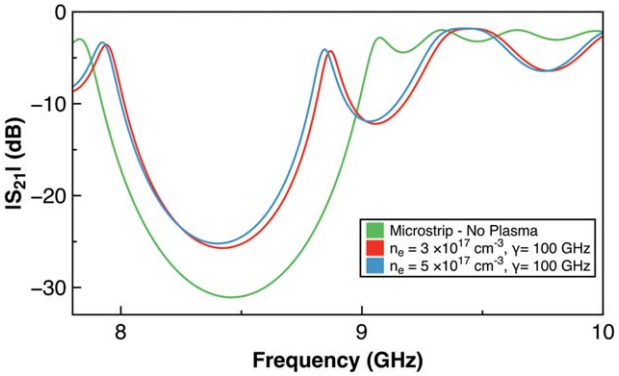

FIGURE 5 Simulated S_{21} for the PBG microstrip for no plasma and plasma densities $n_e = 3 \times 10^{17}\text{cm}^{-3}$ and $5 \times 10^{17}\text{cm}^{-3}$. [Color figure can be viewed at wileyonlinelibrary.com]

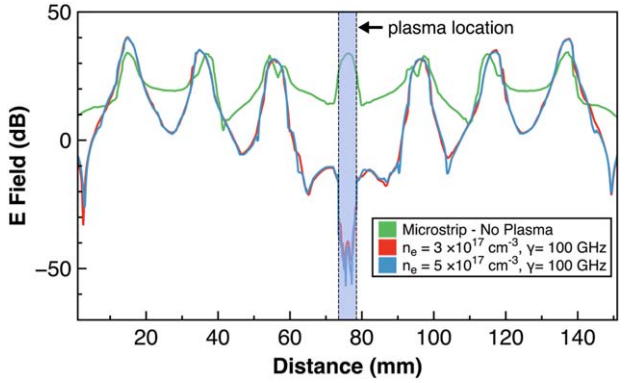

FIGURE 7 Cross sectional E field of the lower ground plane of the microstrip with and without plasma in the center hole. [Color figure can be viewed at wileyonlinelibrary.com]

simulations reproduce the general qualitative behavior seen in the experiments. The bandgap transmission is not as broad (or flat) as that seen in the experiments, but the results confirm that at plasma conditions that are quite realizable, a 10 dB increase in the midgap and in the upper frequency band edge structure can be obtained by filling the central cavity with a high density plasma. We see that slight variations in the plasma density produce only very small changes in transmission when the plasma density is above $n_e = 3 \times 10^{17}\text{cm}^{-3}$. A more quantitative comparison between the experimental measurements and the simulations would require a more detailed description of the spatial and temporal properties of the plasma.

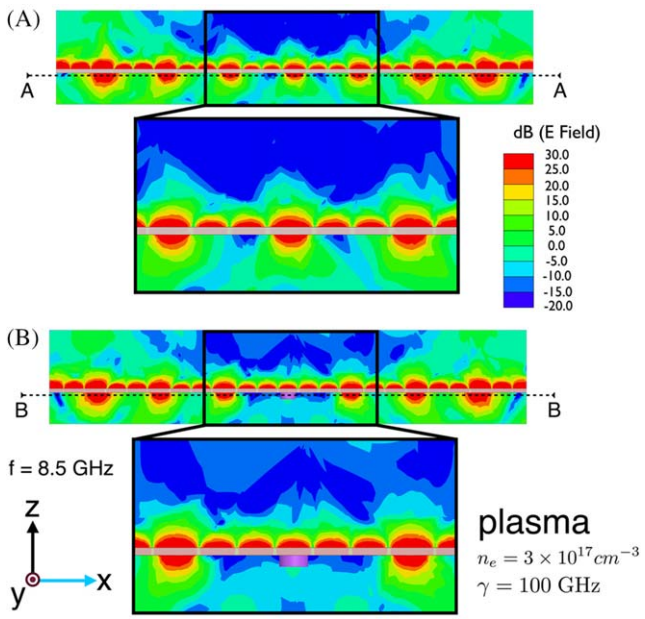

FIGURE 6 Steady state E-field cross section of the PBG microstrip (A) with no plasma in center hole (B) with plasma on in center hole. The dotted lines indicate the location of the E-field cross section in Figure 7. [Color figure can be viewed at wileyonlinelibrary.com]

Figure 6 shows the centerline cross sectional projections over a 150 mm (X) by 20 mm (Z) window of a temporal snapshot of the electric field magnitude above and below the microstrip and the effect of the plasma on the fields in the vicinity of the center PBG cavity. Figure 6A is the case without a plasma, for a frequency centered within the bandgap (8.5 GHz). As expected, we see resonant behavior, with fields extending into and beyond the PBG cavities below the device. The expanded region in Figure 6A zooms in on the region in the vicinity of the central cavity. Figure 6B depicts the same field mapping but with the plasma filling the central cavity. Zooming in on the central cavity, we see that the fields are attenuated (evanescent) where the plasma is located, due to the complex refractive index associated with the negative dielectric constant. This results in stronger and more confined fields on the upper plane of the microstrip and hence greater transmission. Figure 7 plots the electric field magnitude verses propagation direction along the bottom surface of the microstrip (at indicated in Figure 6) at the same instant in time as that in Figure 6. We see that the fields in the center hole are attenuated and reflected with the plasma on, leading to higher field intensity on the signal line and more signal that dissipates out of the ground plane of the PBG cavities.

4 | CONCLUSION

These results demonstrate robust sub-microsecond switching and manipulation of bandgap transmission of a microstrip photonic crystal bandgap device. The use of a pulsed laser source for plasma generation allows for a proof of concept demonstration and convenient experimental measurement of the time response of adding an active element that has a finite decaying lifetime spanning a wide range of electron density. In future studies we aim to explore how such a device can be used as a diagnostic tool for characterizing the

recombination of laser induced plasmas in varying gaseous environments. The device design is also amenable to direct integration of pulsed discharge plasmas, which will afford the possible use of multiple discharges within several of the PBG cavities. Such distributed manipulation of the cavity fields can result in reconfigurable transmission modes without direct manipulation of the signal line. We believe that this manipulation of the radiated fields is a uniquely different form of field control, utilizing the extended field of the ground plane PBG structure to control transmission behavior.

ACKNOWLEDGMENTS

This work was supported in part by a Multidisciplinary University Research Initiative from the Air Force Office of Scientific Research. B.W. and R.C. were also supported in part by a National Defense Science and Engineering Graduate Fellowship.

ORCID

B. Wang http://orcid.org/0000-0002-7192-4249

REFERENCES

[1] Wang B, Cappelli MA. A plasma photonic crystal bandgap device. *Appl Phys Lett.* 2016;108:161101

[2] Radisic V, Qian Y, Coccioli R, Itoh T. Novel 2-D Photonic Bandgap Structure for Microstrip Lines. *IEEE Microwave Guided Wave Lett.* 1998;8:69–71.

[3] Akalin T, Laso MAG, Lopetegi T, Vanb Esien O, Sorolla M, Lippens D. PBG-type microstrip filters with one and two sided patterns. *Microwave Opt Technol Lett.* 2001;30:69–72.

[4] Ouyang J, Cao J, Li S, Peng Z, Li W, Ren W. Application of discharge plasma as dynamic switch in microstrip line. *IEEE Electron Device Lett.* 2010;31:1491–1493.

[5] Cross LW, Member S, Almalkawi MJ, Devabhaktuni VK, Member S. Theory and demonstration of narrowband bent hairpin filters integrated with AC-coupled plasma limiter elements. *IEEE Trans Electromagn Compatibility.* 2013;55:1100–1106.

[6] Thiyagarajan M, Scharer JE. Experimental investigation of 193-nm laser breakdown in air. *IEEE Trans Plasma Sci.* 2008;36:2512–2521.

[7] Thiyagarajan M, Williamson K, Kandi AR. Experimental investigation of 1064-nm IR laser-induced air plasma using optical laser shadowgraphy diagnostics. *IEEE Trans Plasma Sci.* 2012;40:2491–2500.

How to cite this article: Wang B, Lee R, Colon R, Cappelli MA. A microstrip photonic crystal bandgap device with a switchable negative epsilon plasma element. *Microw Opt Technol Lett.* 2017;59:3097–3101. https://doi.org/10.1002/mop.30882

Received: 19 May 2017

DOI: 10.1002/mop.30896

Compact wideband band pass microstrip filter loaded by triangular split ring resonators

Hanane Nasraoui[1,2] | A. D. Capobianco[2] | Ahmed Mouhsen[1] | Jamal El Aoufi[1] | Youssef Mouzouna[1] | Mohamed Taouzari[1]

[1] Laboratory IMII, Faculty of Science and technical Hassan 1 University Settat, Morocco

[2] Photonics and Electromagnetics Group of the Department of Information Engineering at the University of Padova, Italy

Correspondence
Hanane Nasraoui, Laboratory IMII, Faculty of Science and technical Hassan 1 University Settat, Morocco.
Email: hanane.nasraoui@gmail.com

Abstract

A compact wideband band-pass microstrip filter based on triangular split ring resonators is presented. The center frequency of the proposed structure is 3.1 GHz and the 3 dB bandwidth results 1.05 GHz. Good agreements between the simulated and measured results demonstrates the effectiveness of the proposed design. The size of the filter is 14×50 mm^2 only.

KEYWORDS

band-pass filter, metamaterial, microstrip, triangular split ring resonators

1 | INTRODUCTION

It is well known that metamaterial structures, characterized by compact size and light weight, are very attractive for the implementation of novel microwave circuits. These materials are often referred to as left handed or double negative materials: a class of materials whose properties are not found in nature. In 1968, V. G. Veselago theoretically introduced the possibility of having materials with negative refractive index.[1] Pendry et al.[2] presented an artificial material with negative permittivity in the GHz range obtained by means of a trellis of thin metallic wires. In Ref. [3] was proposed for the first time the Split Ring Resonator (SRR) as a basic